ELSEVIER

Biosensors & Bioelectronics 14 (1999) 417–425

BIOSENSORS & BIOELECTRONICS

Protein detection with a novel ISFET-based zeta potential analyzer

Sabine Koch [a,*], Peter Woias [a], Leonhard K. Meixner [a], Stephan Drost [a], Hans Wolf [b]

[a] *Fraunhofer-Institute for Solid State Technology, Hansastrasse 27d, D-80686 Munich, Germany*
[b] *University of Regensburg, D-93053 Regensburg, Germany*

Received 23 February 1998; received in revised form 3 January 1999; accepted 14 January 1999

Abstract

This publication presents a novel ISFET-based measurement concept for the determination of the zeta potential, which is known to be an efficient method for the detection of protein accumulations onto surfaces. The basic set-up consists of two monolithically integrated ISFET sensors arranged in a serial flow configuration together with a precoated fused silica capillary, which provides the reactive surface for the protein detection. In comparison with the state of the art, this novel biosensor system is characterized by a small size, an extremely low reagent consumption, a simple fluidic concept, a short analysis time, and a very effective noise suppression due to the differential ISFET set-up. In the following, an overview is given over the theoretical background of the measurement principle. In order to get deeper insight into the theoretical background of the measurement principle, a simulation model was developed which is based on the site-binding theory and takes into account the different proton dissociation equilibria of the surface groups as well as the influence of monovalent electrolyte ions. A quasi-Newton iteration after Broyden was used for the numerical solution of the formulated equation system. For an experimental confirmation of the simulation results, the calculated zeta potential vs. pH curves were compared with measured data for various modifications of the fused silica capillaries (in untreated state, after a hydrothermal activation, and after the deposition of several silanes) and it could be shown, that the chosen physical model represents a satifactory theoretical basis for the description of the occuring surface effects. Measurements before and after a covalent coupling of the model analyte lysozyme were performed in order to demonstrate the feasibility of an immunosensor based on the measurement of the streaming potential and showed a significant shift of the zeta potential vs. pH curves.

Keywords: Zeta potential; ISFET; Fused silica capillary; Immunosensor; Site-binding model

1. Introduction

After numerous experimental trials (Meixner and Koch, 1992; Eijkel, 1995) and a detailed theoretical analysis (Schasfoort, 1989; Meixner and Koch, 1992; Eijkel, 1995) it is obvious today, that the direct detection of protein charges via potentiometric sensors in general, and the ion sensitive field effect transistor (ISFET) in particular, is hindered by severe physical limitations, which prevent the often-proposed application as a direct immunosensor.

In this situation the evaluation of electrokinetic effects can serve as an alternative to the 'classical' measurement under thermodynamic equilibrium conditions. The measurement of the streaming potential or the zeta potential, respectively, represents a well-established analytical method for the characterization of electrochemical surface properties. In particular, the adsorption or desorption of various substances at a certain surface, or the alteration of a surface during a chemical or physical process can be monitored directly and on-line (Klason et al., 1991). Important fields of application can be seen in material biocompatibility tests for medical devices or the characterization of clothing material properties in the textile industry. Apart from these established fields of application, the detection of antigen–antibody reactions taking place at a solid–liquid interface has been the focus of various approaches to immunosensors based on the streaming potential principle (Glad et al.,

* Corresponding author. Tel.: +49-89-54759222; fax: +49-89-54759100.

0956-5663/99/$ - see front matter
PII: S0956-5663(99)00008-1

1986). Most of this work is concentrating on the development and optimization of the biochemical receptor layers; beside that, little has been done up to now to further improve the measurement set-up for the potential recording, which in most cases uses two glass reference electrodes located at both ends of a flow-through reaction cartridge.

This publication presents a novel method for the detection of the streaming potential, which is based on ISFET instead of glass electrodes for the recording of the occuring potential differences. The set-up uses a flow-through system with two monolithically integrated ISFET sensors located at the beginning and the end of a fused silica capillary, which acts as a flow pathway. A metal electrode is located at the beginning of the flow pathway to supply the reference potential close to the first ISFET sensor. Thus, the streaming potential drop across the capillary is added as an offset to the signal of the second ISFET sensor and can be directly extracted by operating both ISFETs in a differential measurement configuration. In comparison with the conventional set-up described above, this approach offers the following advantages:

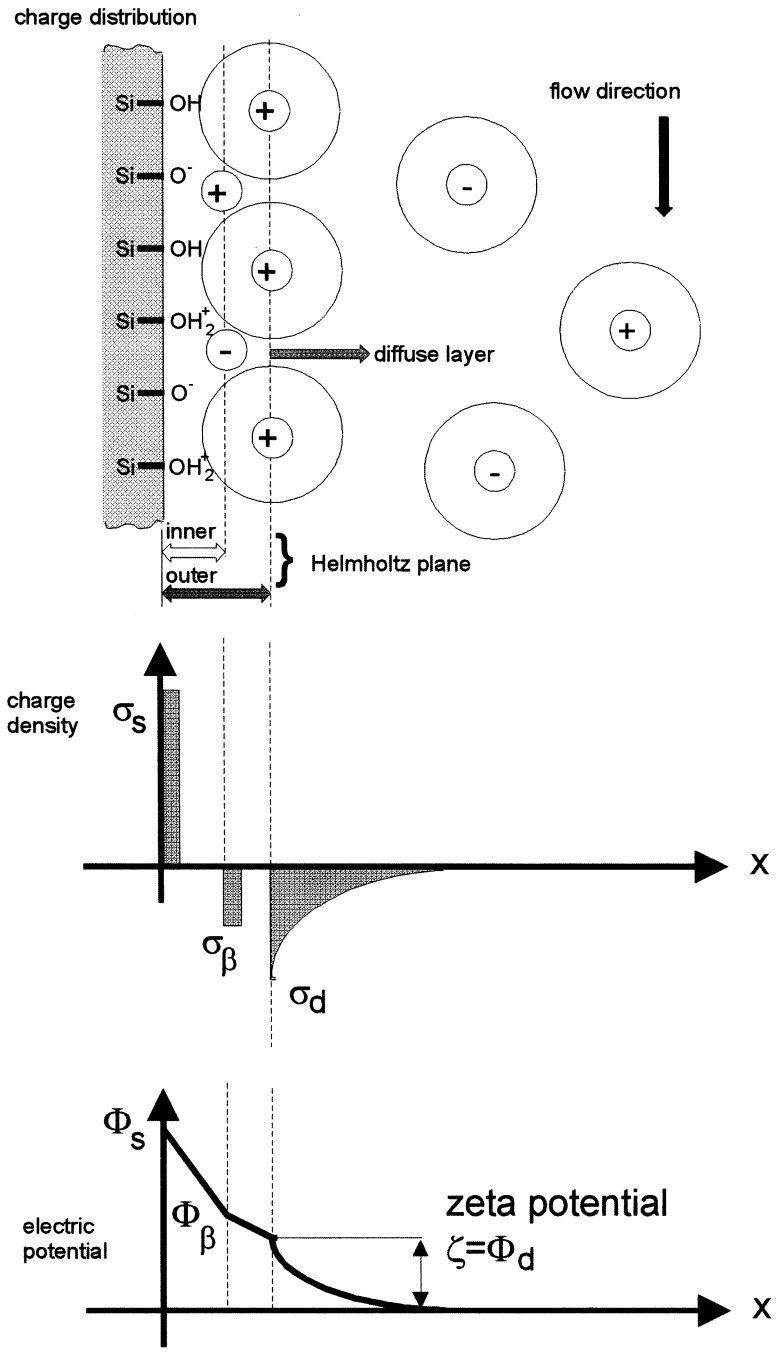

Fig. 1. Charge and potential distribution at a solid–liquid interface; definition of the zeta potential.

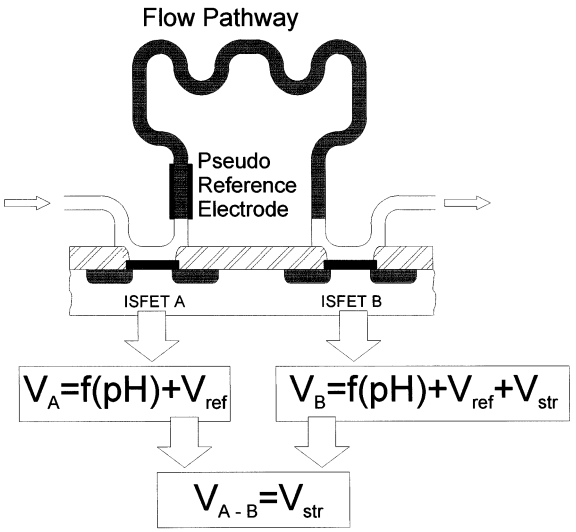

Fig. 2. Measurement of the streaming potential by means of an ISFET differential set-up.

1. In contrary to a glass electrode, an ISFET is a robust and maintenance-free device.
2. Due to the well-established processes of semiconductor fabrication, monolithic ISFET sensor arrays are available with almost identical electric and electrochemical properties. Therefore, all common mode disturbances, such as temperature effects, electrochemical short term and long term instabilities (i.e. drift and slow response), pH-sensitivity and ion cross sensitivity can be eliminated by the differential measurement set-up (Woias et al., 1993; Woias, 1994).
3. The electrochemical potential of the metal reference electrode can as well be considered to be an electrical common mode disturbance; therefore, the necessity of a conventional glass reference electrode with all its drawbacks does no longer exist.
4. Because of the high degree of miniaturization feasible with ISFET sensors, the whole system can be effectively reduced in terms of flow rate and reagent consumption.

For an immunosensor application, a suitable receptor layer is immobilized at the inner surface of the capillary. The specific binding of the belonging reaction partner is accompanied by a shift of the streaming potential, which directly can be recorded by the ISFET sensors.

2. Theory

According to the well-known site-binding theory (Yates et al., 1974), an anisotropic ion accumulation exists at the contact interface between an electrochemically active surface and a liquid electrolyte (Fig. 1). Due to their different size and charge the ions form a well-confined electric double layer close to the surface, and, according to the Gouy–Chapman theory (Bard and Faulkner, 1980), a diffuse layer of counter charges between the Helmholtz planes and the neutral bulk of the solution. Whereas the Helmholtz planes are strongly adsorbed, the diffuse layer is much more mobile and, therefore, can be displaced by an outward force.

Therefore, mainly the part of the double layer closest to the interface will be retained by the surface, if the liquid phase is caused to flow relative to the surface in the direction indicated by the arrow in Fig. 1. Due to the resulting local distortion of the charge balance, a continuous ion separation takes place between the mobile and the attached part of the double layer. A flow of excess ions is the consequence, which creates a potential difference in flow direction. Fig. 1 also shows the potential distribution from the interface towards the bulk of the solution. The potential difference V_{str}, which can be measured from one end of the flow pathway to the other, depends on the potential that is defined at the outer Helmholtz plane: the zeta potential ζ. Under the assumption of a laminar flow and a

Table 1
Summary of the simulation parameters

Parameter	Untreated capillary	Hydrothermally activated capillary	Aminosilanized capillary
pK_1	1.4	1.4	1.4
pK_2	4.6	4.6	4.6
pK_3	–	–	10.0
$pK_{11} = pK_{22}$	2.0	2.0	0.5
pK_{33}	–	–	0.5
N_0 (per m^2)	5×10^{18}	8×10^{18}	8×10^{18}
$N_{amino}/N_{silanol}$	–	–	0.2
C_1 (F/m^2)	1.25	1.25	1.25
C_2 (F/m^2)	0.2	0.2	0.2
c^e (M)	0.01	0.01	0.01
ε_r	80	80	80
T (K)	300	300	300

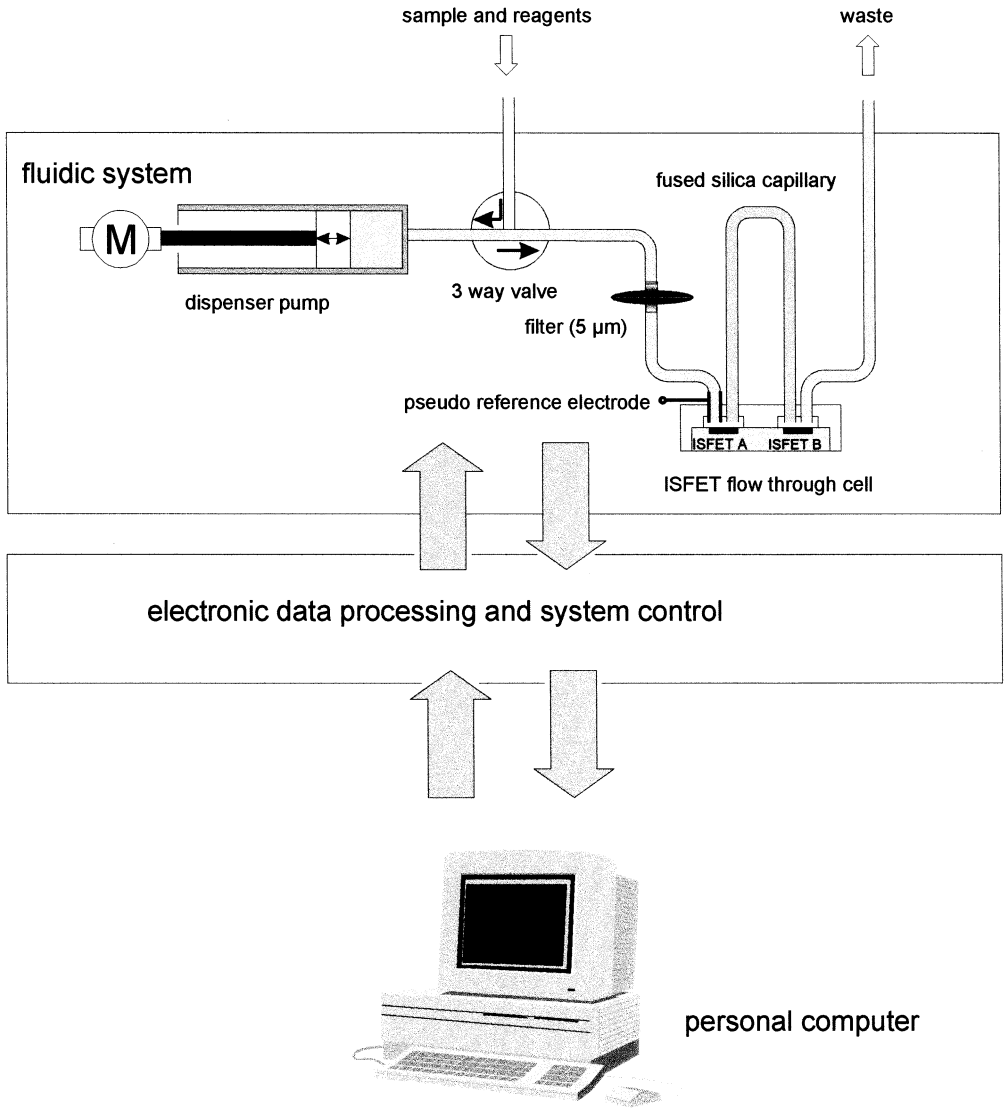

Fig. 3. Schematic drawing of the measurement set-up.

negligible surface conductance, the correlation between V_{str} and the zeta potential is given by the Helmholtz–Smoluchowsky equation (Bousse et al., 1992):

$$\zeta = \frac{\eta \lambda V_{str}}{\varepsilon \varepsilon_0 \Delta p} \quad (1)$$

where ζ is the zeta potential (V); η, the dynamic viscosity (Pa s); ε, the relative dielectric constant of the fluid; $\varepsilon_0 = 8.854187817 \times 10^{-12}$ (F/m); λ, the specific conductivity (S/m); V_{str}, the measured streaming potential (V); Δp, the pressure difference (Pa).

For the capillary used as a flow pathway in this study, the pressure drop Δp and the flow rate Q through the capillary are related by Hagen–Poiseuille's law (Mende and Simon, 1981):

$$\Delta p = \frac{8 Q l \eta}{R^4 \pi} \quad (2)$$

where Q is flow rate (m^3/s), l, the length of the capillary (m); η, the dynamic viscosity (Pa s); R, the radius of the capillary (m).

The hydronium ion concentration as well as that of all other species present in the solution influence the streaming potential V_{str} by either changing the physical characteristics (conductivity λ, dielectric constant ε) or by affecting the zeta potential ζ, e.g. via adsorption to the solid surface.

As shown in Fig. 2, the measurement set-up consists of a fused silica capillary, which acts as a flow pathway, and two ISFETs mounted at the beginning and the end of the capillary. The flow rate is controlled by means of a precision piston dispenser pump in the direction indicated by the arrows. The reference potential is defined by a stainless steel electrode which is located near the first ISFET sensor B at the beginning of the capillary. Due to the physical effects described above,

the potential drop V_{str} is formed along the flow pathway and is added to the signal of ISFET A. Due to its location near the reference electrode, ISFET B only measures the zero potential $f(pH) + V_{ref}$ of the set-up, which is also part of the signal of ISFET A. Thus, the difference of both sensor signals directly yields the streaming potential V_{str}.

3. Simulation model

For the description of charge and potential at the oxide–electrolyte interface different models can be used. A common feature of all these models is the idea of dissociable surface groups and the formulation of similar mass action laws and balance equations. The basic difference of these models can be seen in the structure of the resulting electrical double layer. Westall and Hohl discuss the following concepts (Westall and Hohl, 1980): the model of a constant capacity, the model of a diffuse layer, the Stern model after Bowden for a AgI-electrode, the Stern model in its original version (Hg-electrode), and the triple layer model after Yates and Davis (Yates et al., 1974; Davis et al., 1978).

The so-called triple layer is considered to be the best tool for a quantitative description of electrokinetic potentials and was used in this study—together with the site-binding theory for the surface charge—for the calculation of charge and potential at the fused silica capillary. The formulation of the equation system follows mostly Yates and Davis (Yates et al., 1974; Davis et al., 1978).

Based on this equation system, the charge and potential values and—applying Eq. (1)—the measurable streaming potential can be determined numerically as a function of the electrolyte composition and the surface structure of the capillary. Thus, changes in the surface structure of the capillary can be interpreted by evaluating the measured changes of the streaming potential curves.

For the calculation of the conditions at the inner surface of an uncoated fused silica capillary the equations for the equilibrium constants of silanol groups have been used. In this case, the total amount of reactive silanol groups is directly dependent on the surface modification (untreated or hydrothermally activated). The influence of additional reactive amino groups, which are introduced by coating with an aminosilane, is taken into account by formulating the belonging equlibrium equations for amino groups. A numerical calculation of the conditions after the coating with a lysozyme layer has not been implemented

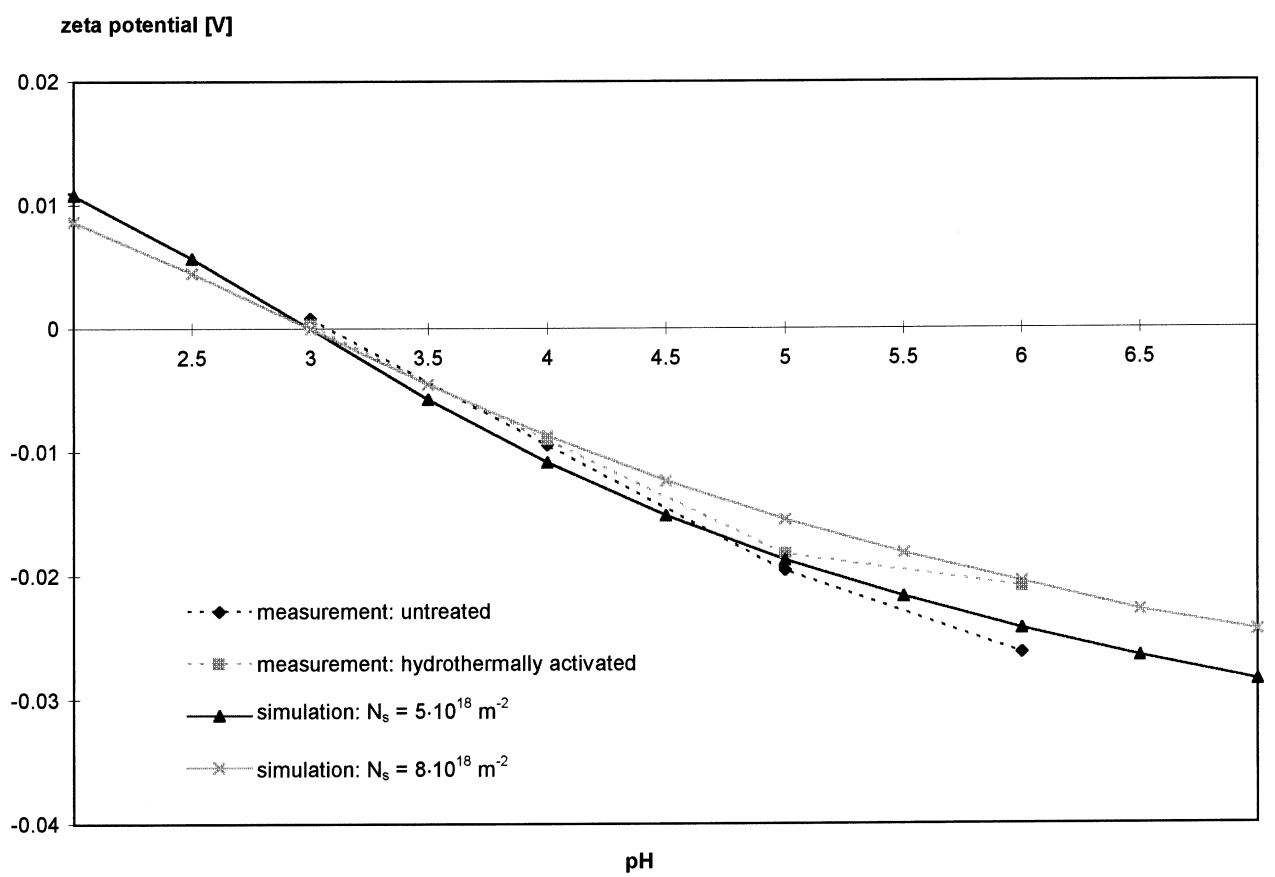

Fig. 4. Measured and calculated zeta potential vs. pH curves for untreated and hydrothermally activated fused silica capillaries.

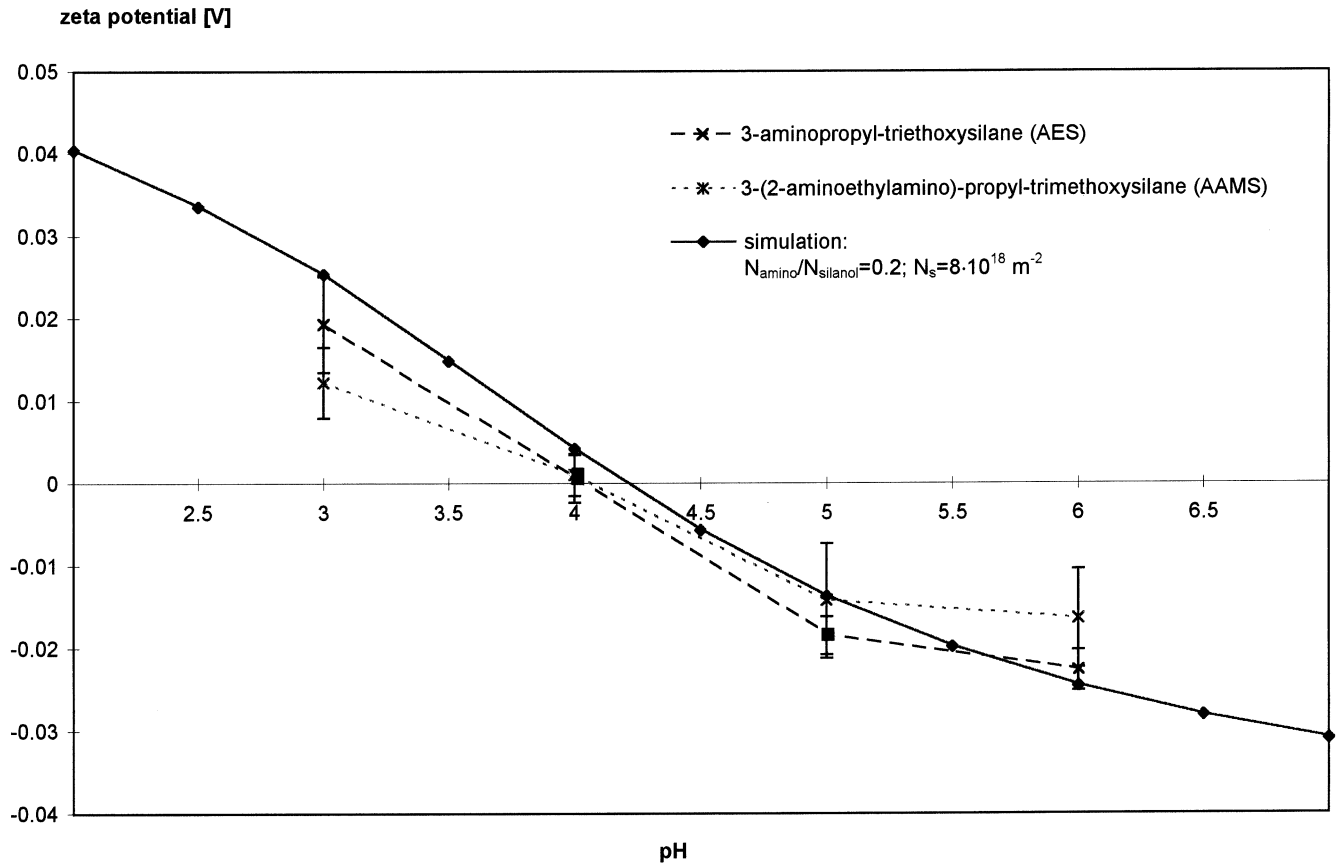

Fig. 5. Measured and calculated zeta potential vs. pH curves for aminosilanized fused silica capillaries.

into the simulation, as the equilibrium constants of the reactive side groups at such a protein depend extremely on the sterical conditions of the immobilized layer and thus cannot be given in the same way as for the silanol and amino groups.

In the case of silicon dioxide which is in direct contact with an electrolyte solution, the surface charge at the SiO_2–electrolyte interface originates from the dissociation of silanol groups. Due to their amphoteric character, they can act either as a proton acceptor or donator, i.e. as a Brønsted base or acid. For the simulation the mass action laws for these reactions have to be formulated. When assuming a Boltzmann correlation between the bulk concentration and the surface concentration of the hydronium ions, the equations can be written as follows:

$$K_1 = \frac{[\mathrm{SiOH}]\cdot[\mathrm{H^+}]}{[\mathrm{SiOH_2^+}]}\cdot\exp\left(-\frac{e\Phi_s}{kT}\right) \quad (3)$$

$$K_2 = \frac{[\mathrm{SiO^-}]\cdot[\mathrm{H^+}]}{[\mathrm{SiOH}]}\cdot\exp\left(-\frac{e\Phi_s}{kT}\right) \quad (4)$$

where K_i is the equilibrium constant of reaction i; Φ_s, the surface potential (V, see Fig. 1); k, the Boltzmann factor $= 1.380662\times10^{-23}$ (J/K); T, the absolute temperature (K).

In order to take into account the adsorption of salt ions (here for example K^+ and Cl^-) from the electrolyte, the following equations can be written for the equilibrium constants as a function of the potential Φ_β at the inner Helmholtz plane (see Fig. 1) where the counter ions are assumed to be located (Smit and Holten, 1980).

$$K_{11} = \frac{[\mathrm{SiOH_2^+}]\cdot[\mathrm{Cl^-}]}{[\mathrm{SiOH_2^+Cl^-}]}\cdot\exp\left(+\frac{e\Phi_\beta}{kT}\right) \quad (5)$$

$$K_{22} = \frac{[\mathrm{SiO^-}]\cdot[\mathrm{K^+}]}{[\mathrm{SiO^-K^+}]}\cdot\exp\left(-\frac{e\Phi_\beta}{kT}\right) \quad (6)$$

where Φ_β is the potential at the inner Helmholtz plane (V, see Fig. 1).

As the total amount of reactive surface groups N_s does not change, the following equation can be formulated:

$$N_s = [\mathrm{SiOH}] + [\mathrm{SiO^-}] + [\mathrm{SiOH_2^+}] + [\mathrm{SiO^-K^+}] + [\mathrm{SiOH_2^+Cl^-}] \quad (7)$$

The concentrations of those surface groups associated with an electrolyte ion are taken into account here, because this structure is interpreted as a dipole and not as an electrically neutral molecule.

The charge density at the solid surface σ_s can be calculated from the total amount of charged surface groups:

$$\sigma_s = e \cdot ([SiOH_2^+] + [SiOH_2^+ Cl^-] - [SiO^-] - [SiO^- K^+]) \quad (8)$$

The charge density at the inner Helmholtz plane σ_β is determined by the total concentration of adsorbed electrolyte ions:

$$\sigma_\beta = e \cdot ([SiO^- K^+] - [SiOH_2^+ Cl^-]) \quad (9)$$

Due to the demand of charge neutrality in a stationary equilibrium, all charge densities depicted in Fig. 1 must compensate each other:

$$\sigma_s + \sigma_\beta + \sigma_d = 0 \quad (10)$$

After the triple layer model for 1:1 electrolytes, the potentials occurring at the different layers (see Fig. 1) can be correlated to their respective charge densities via the Eqs. (11)–(13) (Yates et al., 1974; Davis et al., 1978; Fung et al., 1986):

$$\Phi_d = \zeta = \frac{2kT}{e} \cdot ar \sin h\left(\frac{\sigma_d}{\sqrt{8 \cdot \varepsilon_r \varepsilon_0 \cdot kT \cdot c^e}}\right) \quad (11)$$

$$\Phi_s - \Phi_\beta = \frac{\sigma_s}{C_1} \quad (12)$$

$$\Phi_\beta - \Phi_d = \frac{-\sigma_d}{C_2} \quad (13)$$

C_1 and C_2 signify the capacitances at the inner and outer Helmholtz plane, respectively, and can be assumed to be constant in a first approximation (Johansson and Norberg, 1968); $c^e = c^+ = c^-$ means the concentration of the electrolyte.

From these basic equations the expressions for the concentrations of the different charged groups can be derived as a function of N_s, Φ_s, and the dissociation constants (Koch, 1997). For the numeric evaluation starting values for the potentials Φ_s and Φ_β are given for which the concentrations of the charged groups can be determined at a certain pH value and electrolyte concentration. Equilibrium constants and double layer capacitances are taken from literature. With the help of Eqs. (8)–(10) the charge densities σ_s, σ_β, and σ_d are calculated. Eq. (11) yields the value for the zeta potential. Using Eqs. (12) and (13), the values of Φ_s and Φ_β can be determined; are they consistent with the starting values within a preset accuracy, the calculation is finished. Otherwise, the starting value is adjusted and the above described steps are repeated. This procedure is reiterated until the convergence criterion is reached.

For the solution of the equation system, the Broyden method has been used as described by Press (Press et al., 1992).

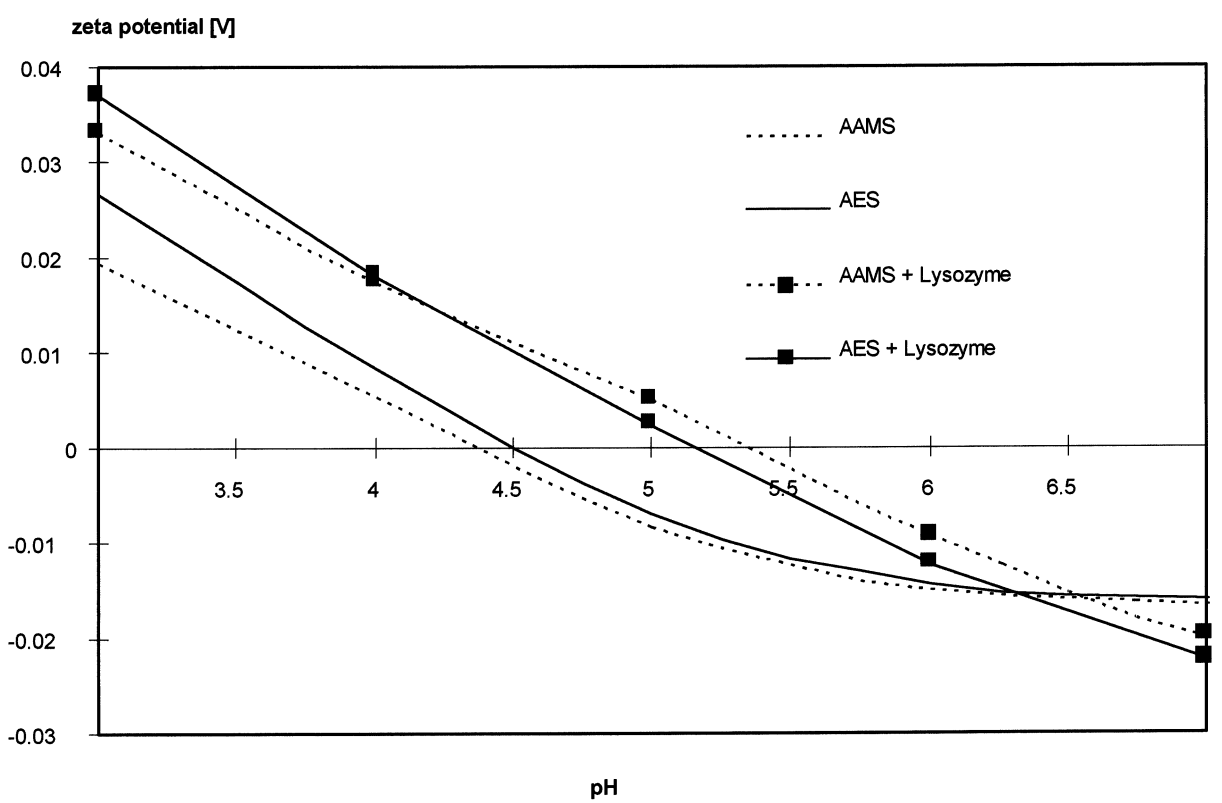

Fig. 6. The effect of lysozyme coupling to silanized fused silica capillaries (treatment as described above).

In this way the potentials and charge distributions are determined for each pH value from pH 2 to 9. From these data the zeta potential curves as a function of the pH value can be simulated.

Analogously, the coating with an aminosilane can be simulated by substituting amino groups for a certain amount of silanol groups. In this case, the following additional equations have to be considered:

$$K_3 = \frac{[RNH_2]\cdot[H^+]}{[RNH_3^+]}\cdot\exp\left(-\frac{e\Phi_s}{kT}\right) \quad (14)$$

$$K_{33} = \frac{[RNH_3^+]\cdot[Cl^-]}{[RNH_3^+Cl^-]}\cdot\exp\left(+\frac{e\Phi_\beta}{kT}\right) \quad (15)$$

$$N_{silanol} = [SiOH] + [SiO^-] + [SiOH_2^+] + [SiO^-K^+] + [SiOH_2^+Cl^-] \quad (16)$$

$$N_{amino} = [RNH_2] + [RNH_3^+] + [RNH_3^+Cl^-] \quad (17)$$

The total amount of surface groups is now given as the sum of silanol and amino groups:

$$N_s = N_{silanol} + N_{amino} \quad (18)$$

Using the measured data and comparing various literature data (Dugger et al., 1964; Davis et al., 1978; Bousse and Meindl, 1986; Fung et al., 1986; Harame et al., 1987; Hair, 1988; Hiemstra et al., 1989a,b; Vlasov et al., 1990; Rosen et al., 1993) the following set of parameters (Table 1) fitted the experimental results best and were used for all simulations shown here.

4. Experimental

For the experiments, standard GC capillaries with a length of 30 cm were used (SUPELCO, i.d. 0.25 mm). After a first control measurement with the untreated capillaries, the measurement set-up shown above was characterized by subsequentially generating and monitoring the following surface modifications:

1. Hydrothermal activation by thermal treatment of the sealed capillaries, which were previously filled with KOH solution.
2. Silanization with 3-(2-aminoethylamino)-propyltrimethoxysilane (AAMS) or 3-aminopropyl-triethoxysilane (AES), respectively. This was done by incubating with an aqueous 5% per vol. silane solution overnight at 80°C (Weetall and Filbert, 1974).

For all measurements, citrate buffer was prepared in a pH range from pH 3 to 8 by mixing the appropriate amounts of 10 mM citric acid and 10 mM Na_2HPO_4.

In order to demonstrate that the covalent binding of a protein layer can be monitored with this measurement set-up, lysozyme was coupled to the silanized capillaries by first incubating for 2 h with a 2.5% per vol. glutardialdehyde solution in PBS and, subsequently, for 15 h with a solution of 10 mg/ml lysozyme in a buffer at pH 7 (Weetall and Filbert, 1974).

The ISFET sensors used in this study were designed and fabricated in cooperation with the Fraunhofer-Institute for Solid State Technology, Munich and have already been described in a number of publications (Müller, 1993; Hein, 1994).

The complete measurement set-up is depicted in Fig. 3. In order to obtain the zeta potential vs. pH curves which are shown in the next paragraph, the streaming potential V_{str} first was recorded for each pH value with flow rates of 1, 2, 3 and 4 ml/min. By computing a linear regression the gradient $\Delta V_{str}/\Delta p$ was obtained from these data and used to calculate the zeta potential ζ according to Eqs. (1) and (2). The dynamic viscosity η and the electrical conductivity λ were obtained by separate measurements, ε was set to a value of 80.

5. Results

Fig. 4 shows the comparison between measured and calculated data for untreated and hydrothermally activated capillaries. As a result one can recognize the following characteristics:

1. The zeta potential of all capillaries is decreasing with an increase of pH; this result is in agreement with zeta potential measurements described in the literature (Bousse et al., 1991).
2. The hydrothermal activation (i.e. the enhancement of the amount of silanol groups) showed no shift of the point of zero zeta potential in comparison with the untreated capillary. Only the gradient of the measured curve was reduced. The comparison with the simulated curves shows an increase of the silanol groups from $N_s = 5\times10^{18}$ to 8×10^{18} per m^2 after the activation.

The effect of additional amino groups on the measured and simulated curves is shown in Fig. 5. As a result, the following items can be summarized:

1. The point of zero zeta potential is shifted to increasing pH values due to the coating of the capillaries, from starting with pH 3.0 for a hydrothermally activated capillary, to about pH 4.0 for capillaries coated with AES or AAMS.
2. From the calculated values a ratio of $N_{amino}/N_{silanol} = 0.2$ (assuming a total amount of surface groups of $N_s = 8\times10^{18}$ per m^2) can be derived.
3. In general, the reproducibility of the measurement is best for untreated and hydrothermally activated capillaries. During the subsequent steps, an increasing spread-up of the zeta potential curves is observed; the trend of the zero shift, however, was obtained in a large number of measurements, indicating the validity of the data presented in Fig. 5.

Thus, the foregoing experimental and theoretical studies could demonstrate that the chosen site binding model represents a realistic basis for the description of the surface effects at a fused silica capillary and the resulting streaming potential.

Fig. 6 shows the effect of covalently bound lysozyme on the measured zeta potential: the point of zero potential is shifted to a significantly higher value (up to pH 5.4) in comparison with the silanized capillary (about pH 4.5).

6. Discussion and outlook

In this previous investigation, the feasibility of streaming potential measurements with ISFET sensors has been demonstrated. It could be shown, that this novel measurement principle offers various advantages in comparison with commercially available systems.

Experiments concerning the detectability of protein adsorption suggest the feasibility of an immunosensing unit based on the measurement of the streaming potential by means of the described ISFET set-up. However, a deeper understanding of the electrochemical mechanisms is still necessary.

Future investigations will use an immobilized receptor layer for the detection of the belonging biomolecule. Due to the enormous miniaturization potential of this method, in near future small, even portable analysis systems can be realized, which require only minute analyte volumes and can be used for on-line monitoring in various fields of application. Beside a more compact design of the already realized capillary reactor, also a micro-miniaturized silicon channel structure can be used as a second-generation reactor (Woias et al., 1996).

References

Bard, A.J., Faulkner, L.R., 1980. Electrochemical methods, fundamentals and applications. Wiley, New York.

Bousse, L.J., Meindl, J.D., 1986. Surface potential pH characteristics in the theory of the oxide–electrolyte interface. in: Davis, J.A., Hayes, K.F. (Hrsg.), Geochemical Processes at Mineral Surfaces, Am. Chem. Soc., Washington, DC 79–98, ACS Symposium Series No. 323.

Bousse, L.J., Mostarshed, S., Van der Shoot, B., De Rooij, N.F., Gimmel, P., Göpel, W., 1991. Zeta potential measurements of Ta_2O_5 and SiO_2 thin films. J. Colloid Interface Sci. 147, 22–32.

Bousse, L.J., Mostarshed, S., Hafeman, D., 1992. Combined measurement of surface potential and zeta potential at insulator/electrolyte interfaces. Sens. Actuators B 10, 67–71.

Davis, J.A., James, R.O., Leckie, J.O., 1978. Surface ionisation and complexation at the oxide/water interface. J. Colloid Interface Sci. 63 (3), 480–499.

Dugger, D.L., Stanton, J.H., Irby, B.N., McConnell, B.L., Cummings, W.W., Maatman, R.W., 1964. The exchange of twenty metal ions with the weakly acidic silanol group of silica gel. J. Phys. Chem. 68 (4), 757–760.

Eijkel, J., 1995. Potentiometric detection and characterization of adsorbed protein using stimulus—response measurement techniques. PhD Thesis, University of Twente, Enschede.

Fung, C.D., Cheung, P.W., Ko, W.H., 1998. A generalized theory of an electrolyte–insulator–semiconductor fieldeffect transistor. IEEE Trans. Electron Devices ED-33 (1), 8–18.

Glad, C., Sjödin, K., Mattiasson, B., 1986. Streaming potential—a general affinity sensor. Biosensors 2, 89–100.

Hair, M.L., 1988. The acidity of silica surfaces. Silicon Chemistry, Chichester, pp. 481–489.

Harame, D.L., Bousse, L.J., Shott, J.D., Meindl, J.D., 1987. Ion-sensing devices with silicon nitride and borosilicate glass insulators. IEEE Trans. Electron Devices ED-34 (8), 1700–1707.

Hein, P., 1994. Ionensensitive Feldeffekttransistoren—Halbleitertechnologie, Entwurf und Verifikation. PhD Thesis, Technical University, Munich.

Hiemstra, T., Van Riemsdijk, W.H., Bolt, G.H., 1989a. Multisite proton adsorption modeling at the solid/solution interface of (hydr)oxides: a new approach I. Model description and evaluation of intrinsic reaction constants. J. Colloid Interface Sci. 133 (1), 91–104.

Hiemstra, T., De Wit, J.C.M., Van Riemsdijk, W.H., 1989b. Multisite proton adsorption modeling at the solid/solution interface of (hydr)oxides: a new approach ii. application to various important (hydr)oxides. J. Colloid Interface Sci. 133 (1), 105–117.

Johansson, G., Norberg, K., 1968. Dynamic response of the glass electrode. J. Electroanal. Chem. Interfacial Electrochem. 18, 239–250.

Klason, C., Kubát, J., Quardat, O., 1991. Relation between electrical noise generated during capillary flow of aqueous Poly(ethylene oxide) solutions and streaming potential. Noise in Physical Systems and 1/f Fluctuations, 141–144.

Koch, S., 1997. Messung von Strömungspotentialen mittels Ionensensitiver Feldeffekttransistoren. PhD Thesis, Technical University, Munich, Herbert Utz Verlag Wissenschaft, München.

Meixner, L.K., Koch, S., 1992. Simulation of the ISFET operation based on the site binding model. Sens. Actuators B 6, 315–318.

Mende, D., Simon, G., 1981. Physik-Gleichungen und Tabellen VEB. Fachbuchverlag, 7., neubearb. Auflage, Leipzig.

Müller, E., 1993. Ionensensitive Feldeffekttransistoren mit integrierten CMOS-Schaltungskomponenten zur Signalaufbereitung. PhD Thesis, Technical University, Munich.

Press, W.H., Teukolsky, S.A., Vetterling, W.T., Flannery, B.P., 1992. Numerical recipes in C; the art of computing, 2nd edition. Cambridge University Press.

Rosen, L.A., Baygents, J.C., Saville, D.A., 1993. The interpretation of dielectric response measurements on colloidal dispersions using the dynamic stern layer model. J. Chem. Phys. 98 (5), 4183–4194.

Schasfoort, R.B.M., 1989. A New approach to immunofet operation. PhD Thesis, University Twente, Enschede.

Smit, W., Holten, C.L.M., 1980. Zeta-Potential and radiotracer adsorption measurements on EFG α-AL2O3 single crystals in NaBr solutions. J. Colloid Interface Sci. 78 (1), 1–14.

Vlasov, Y., Bratov, A., Sidorova, M., Tarantov, Y., 1990. Investigation of pH-sensitive ISFETs with oxide and nitride membranes using colloid chemistry methods. Sens. Actuators B 1, 357–360.

Weetall, H.H., Filbert, A.M., 1974. Porous glass for affinity chromatography applications. Methods Enzymol. 34, 59.

Westall, J., Hohl, H., 1980. A comparison of electrostatic models for the oxide/solution interface. Adv. Colloid Interface Sci. 12, 265–294.

Woias, P., Koch, S., Müller, E., Barrow, D., Cefai, J., Curtis, G., Hughes, H., 1993. An ISFET-FIA sytem for high precision pH-recording. Sens. and. Actuators B 15–16, 68–74.

Woias, P., 1994. Ionensensitive Feldeffekttransistoren als Messwandler in chemischen Analysensystemen auf Fliessinjektionsbasis. PhD Thesis, Technical University, Munich.

Woias, P., Richter, M., Yacoub-George, E., Wolf, H., Abel, Th., 1996. A Silicon micromachined open tubular reactor for immunosensor applications. Contribution to the International Conference 'EUROSENSORS X', Leuven, 8.–11.9.1996.

Yates, D.E., Levine, S., Healy, T.W., 1974. Site-binding model of the electrical double layer at the oxide/water interface. J. Chem. Soc. Faraday. Trans. I 1 (70), 1807–1818.